Research Article | Vol. 7, No. 2 | 1 Feb 2017 | OPTICAL MATERIALS EXPRESS 627

Optical Materials EXPRESS

Quantification of non-stoichiometry in YAG ceramics using laser-induced breakdown spectroscopy

S. J. PANDEY,[1] M. MARTINEZ,[2,3] F. PELASCINI,[4] V. MOTTO-ROS,[5] M. BAUDELET,[2,3] AND R. M. GAUME[6, 7, *]

[1]*Department of Physics, University of Central Florida, 4111 Libra Drive, Orlando, FL 32826, USA*
[2]*National Center for Forensic Science, University of Central Florida, 12354 Research Pkwy, Orlando, FL 32826, USA*
[3]*Department of Chemistry, University of Central Florida, 4111 Libra Drive, Orlando, FL 32826, USA*
[4]*CRITT Matériaux Alsace, 19 rue de Saint Junien CS 80023, Schiltigheim cedex 67305, France*
[5]*Institut Lumière Matière, UMR 5306 Université Lyon 1-CNRS, Université de Lyon, 69622 Villeurbanne cedex, France*
[6]*The College of Optics and Photonics, University of Central Florida, 4304 Scorpius St., Orlando FL 32816, USA*
[7]*NanoScience Technology Center, University of Central Florida, 12760 Pegasus Drive, Orlando, FL 32816 USA*
[*]*gaume@ucf.edu*

Abstract: Strict control of composition is of paramount importance for the reproducible fabrication of advanced ceramics. In particular, the preparation of high-grade transparent ceramics of definite line-compounds requires that the ratio of major constitutive elements be quantified with a precision better than a fraction of a mole percent to prevent the precipitation of secondary phases and the scattering of light. Such a requirement poses difficult challenges to most analytical methods, especially when applied to nearly-stoichiometric insulating phases. In this work, we show that laser-induced breakdown spectroscopy (LIBS) is a well-suited technique for the assessment of non-stoichiometry in yttrium aluminum garnet (YAG) ceramics and that the aluminum to yttrium ratio can be determined with a resolution of 0.3 mol %, well within the phase boundaries of YAG.

OCIS codes: (300.6365) Spectroscopy, laser induced breakdown; (160.3380) Laser materials.

References and links

1. G. Ma, T. Shimura, and H. Iwahara, "Ionic conduction and nonstoichiometry in $Ba_x Ce_{0.90} Y_{0.10} O_{3-\alpha}$," Solid State Ion. **110**(1-2), 103–110 (1998).
2. Q. He, Q. Hao, G. Chen, B. Poudel, X. Wang, D. Wang, and Z. Ren, "Thermoelectric property studies on bulk TiO_x with x from 1 to 2," Appl. Phys. Lett. **91**(5), 052505 (2007).
3. E. Breckenfeld, Z. Chen, A. R. Damodaran, and L. W. Martin, "Effects of nonequilibrium growth, nonstoichiometry, and film orientation on the metal-to-insulator transition in $NdNiO_3$ thin films," ACS Appl. Mater. Interfaces **6**(24), 22436–22444 (2014).
4. O. Perner, J. Eckert, W. Häßler, C. Fischer, J. Acker, T. Gemming, G. Fuchs, B. Holzapfel, and L. Schultz, "Stoichiometry dependence of superconductivity and microstructure in mechanically alloyed MgB_2," J. Appl. Phys. **97**(5), 056105 (2005).
5. C. Fujioka, R. Aoyagi, H. Takeda, S. Okamura, and T. Shiosaki, "Effect of non-stoichiometry on ferroelectricity and piezoelectricity in strontium bismuth tantalate ceramics," J. Eur. Ceram. Soc. **25**(12), 2723–2726 (2005).
6. X. Hao and J. Zhai, "Composition-dependent electrical properties of (Pb, La)(Zr, Sn, Ti) O_3 antiferroelectric thin films grown on platinum-buffered silicon substrates," J. Phys. D Appl. Phys. **40**(23), 7447–7453 (2007).
7. Z. Surowiak, M. F. Kupriyanov, A. E. Panich, and R. Skulski, "The properties of the non-stoichiometric ceramics $(1-x)PbMg_{1/3}Nb_{2/3}O_3$–$(x)PbTiO_3$," J. Eur. Ceram. Soc. **21**(15), 2783–2786 (2001).
8. D. Shima and S. Haile, "The influence of cation non-stoichiometry on the properties of undoped and gadolinia-doped barium cerate," Solid State Ion. **97**(1-4), 443–455 (1997).
9. X. Hao, J. Zhou, and S. An, "Effects of PbO content on the dielectric properties and energy storage performance of $(Pb_{0.97}La_{0.02})(Zr_{0.97}Ti_{0.03})O_3$ antiferroelectric thin films," J. Am. Ceram. Soc. **94**(6), 1647–1650 (2011).

#281218 https://doi.org/10.1364/OME.7.000627
Journal © 2017 Received 21 Nov 2016; revised 20 Jan 2017; accepted 24 Jan 2017; published 30 Jan 2017

Optical Materials EXPRESS

10. T.-J. Park, G. C. Papaefthymiou, A. J. Viescas, Y. Lee, H. Zhou, and S. S. Wong, "Composition-dependent magnetic properties of $BiFeO_3$-$BaTiO_3$ solid solution nanostructures," Phys. Rev. B **82**(2), 024431 (2010).
11. J. A. Moyer, R. Misra, J. A. Mundy, C. M. Brooks, J. T. Heron, D. A. Muller, D. G. Schlom, and P. Schiffer, "Intrinsic magnetic properties of hexagonal $LuFeO_3$ and the effects of nonstoichiometry," APL Mater. **2**(1), 012106 (2014).
12. M. Richardson and R. Gaume, "Transparent ceramics for lasers-a game-changer," Am. Ceram. Soc. Bull. **91**, 30 (2012).
13. A. F. Dericioglu, A. R. Boccaccini, I. Dlouhy, and Y. Kagawa, "Effect of chemical composition on the optical properties and fracture toughness of transparent magnesium aluminate spinel ceramics," Mater. Trans. **46**(5), 996–1003 (2005).
14. L. B. Kong, Y. Huang, W. Que, T. Zhang, S. Li, J. Zhang, Z. Dong, and D. Tang, *Transparent Ceramics* (Springer, 2015).
15. X. Li, X. Mao, M. Feng, J. Xie, B. Jiang, and L. Zhang, "Optical absorption and mechanism of vacuum-sintered ZrO_2-doped Y_2O_3 ceramics," J. Eur. Ceram. Soc. **36**(16), 4181–4184 (2016).
16. H. Eilers, "Fabrication, optical transmittance, and hardness of IR-transparent ceramics made from nanophase yttria," J. Eur. Ceram. Soc. **27**(16), 4711–4717 (2007).
17. J. Sanghera, W. Kim, G. Villalobos, B. Shaw, C. Baker, J. Frantz, B. Sadowski, and I. Aggarwal, "Ceramic Laser Materials," Materials (Basel) **5**(12), 258–277 (2012).
18. S. R. Podowitz, R. M. Gaume, W. T. Hong, A. Laouar, and R. S. Feigelson, "Fabrication and Properties of Translucent SrI_2 and Eu:SrI_2 Scintillator Ceramics," IEEE Trans. Nucl. Sci. **6**, 3827 (2010).
19. A. Krell, J. Klimke, and T. Hutzler, "Transparent compact ceramics: inherent physical issues," Opt. Mater. **31**(8), 1144–1150 (2009).
20. L.-L. Zhu, Z.-J. Zhang, B.-Q. Liu, M.-L. Huang, C.-Y. Wang, H.-H. Chen, Z.-Y. Man, and J.-T. Zhao, "Preparation and characterization of non-stoichiometric yttrium aluminum garnet (YAG) with antisite defects as a potential scintillator," IEEE Trans. Nucl. Sci. **61**(1), 312–315 (2014).
21. A. L. Shluger, K. P. Mckenna, P. V. Sushko, D. M. Ramo, and A. Kimmel, "Modelling of electron and hole trapping in oxides," Model. Simul. Mater. Sci. Eng. **17**(8), 084004 (2009).
22. R. Boulesteix, A. Maître, J.-F. Baumard, Y. Rabinovitch, and F. Reynaud, "Light scattering by pores in transparent Nd:YAG ceramics for lasers: correlations between microstructure and optical properties," Opt. Express **18**(14), 14992–15002 (2010).
23. X. Chen, S. Chen, P.-M. Clequin, W. T. Shoulders, and R. Gaume, "Combustion synthesis of lead oxide nanopowders for the preparation of PMN–PT transparent ceramics," Ceram. Int. **41**(1), 755–760 (2015).
24. C.-H. Lu and Y.-C. Chen, "Sintering and decomposition of ferroelectric layered perovskites," J. Eur. Ceram. Soc. **19**(16), 2909–2915 (1999).
25. J. McCloy and R. Tustison, *Chemical Vapor Deposited Zinc Sulfide* (SPIE Press, 2013).
26. J. Abell, I. Harris, B. Cockayne, and B. Lent, "An investigation of phase stability in the Y_2O_3-Al_2O_3 system," J. Mater. Sci. **9**(4), 527–537 (1974).
27. A. Patel, M. Levy, R. Grimes, R. Gaume, R. Feigelson, K. McClellan, and C. Stanek, "Mechanisms of nonstoichiometry in $Y_3Al_5O_{12}$," Appl. Phys. Lett. **93**(19), 191902 (2008).
28. R. Gaume, Y. He, A. Markosyan, and R. L. Byer, "Effect of Si-induced defects on 1 [micro sign]m absorption losses in laser-grade YAG ceramics," J. Appl. Phys. **111**(9), 093104 (2012).
29. S. Shikao and W. Jiye, "Combustion synthesis of Eu^{3+} activated $Y_3Al_5O_{12}$ phosphor nanoparticles," J. Alloys Compd. **327**(1-2), 82–86 (2001).
30. Y. Wang, G. Baldoni, W. H. Rhodes, C. Brecher, A. Shah, U. Shirwadkar, J. Glodo, N. Cherepy, and S. Payne, "Transparent garnet ceramic scintillators for gamma-ray detection," in *SPIE Optical Engineering + Applications* (International Society for Optics and Photonics 2012), pp. 850717–850717–850718.
31. R. Gaume, D. Steere, and S. Sundaram, "Effect of nonstoichiometry on the terahertz absorption of $Y_3Al_5O_{12}$ optical ceramics," J. Mater. Res. **29**(19), 2338–2343 (2014).
32. V. V. Osiko, *Growth and Defect Structures* (Springer-Verlag, 1984).
33. K.-T. Tsen, M. Baudelet, J.-J. Song, M. Boueri, J. Yu, M. Betz, A. Y. Elezzabi, X. Mao, S. S. Mao, and R. Russo, "Laser ablation of organic materials for discrimination of bacteria in an inorganic background," Proc. SPIE **7214**, 72140J (2009).
34. E. Negre, V. Motto-Ros, F. Pelascini, S. Lauper, D. Denis, and J. Yu, "On the performance of laser-induced breakdown spectroscopy for quantitative analysis of minor and trace elements in glass," J. Anal. At. Spectrom. **30**(2), 417–425 (2015).
35. J. O. Cáceres, J. Tornero López, H. H. Telle, and A. González Ureña, "Quantitative analysis of trace metal ions in ice using laser-induced breakdown spectroscopy," Spectrochim. Acta B At. Spectrosc. **56**(6), 831–838 (2001).
36. R. J. Lasheras, C. Bello-Gálvez, and J. M. Anzano, "Quantitative analysis of oxide materials by laser-induced breakdown spectroscopy with argon as an internal standard," Spectrochim. Acta B At. Spectrosc. **82**, 65–70 (2013).
37. P. Yaroshchyk, R. J. S. Morrison, D. Body, and B. L. Chadwick, "Quantitative determination of wear metals in engine oils using LIBS: The use of paper substrates and a comparison between single- and double-pulse LIBS," Spectrochim. Acta B At. Spectrosc. **60**(11), 1482–1485 (2005).
38. A. P. M. Michel, "Review: applications of single-shot laser-induced breakdown spectroscopy," Spectrochim. Acta B At. Spectrosc. **65**(3), 185–191 (2010).

Optical Materials EXPRESS

39. J. Zhang, G. Ma, H. Zhu, J. Xi, and Z. Ji, "Accurate quantitative analysis of metal oxides by laser-induced breakdown spectroscopy with a fixed plasma temperature calibration method," J. Anal. At. Spectrom. **27**(11), 1903 (2012).
40. H. Estupiñán, D. Y. Peña, Y. O. García, R. Cabanzo, and E. Mejía-Ospino, "Stoichiometry analysis of titanium oxide coating by LIBS," Eur. Phys. J. D **53**(1), 69–73 (2009).
41. A. C. Popescu, S. Beldjilali, G. Socol, V. Craciun, I. N. Mihailescu, and J. Hermann, "Analysis of indium zinc oxide thin films by laser-induced breakdown spectroscopy," J. Appl. Phys. **110**(8), 083116 (2011).
42. J. Gruber, J. Heitz, H. Strasser, D. Bäuerle, and N. Ramaseder, "Rapid in-situ analysis of liquid steel by laser-induced breakdown spectroscopy," Spectrochim. Acta B At. Spectrosc. **56**(6), 685–693 (2001).
43. A. Ikesue, I. Furusato, and K. Kamata, "Fabrication of polycrystalline, transparent YAG ceramics by a solid-state reaction method," J. Am. Ceram. Soc. **78**(1), 225–228 (1995).
44. R. Noll, *Laser-Induced Breakdown Spectroscopy*(Springer, 2012).
45. V. Motto-Ros, E. Negre, F. Pelascini, G. Panczer, and J. Yu, "Precise alignment of the collection fiber assisted by real-time plasma imaging in laser-induced breakdown spectroscopy," Spectrochim. Acta B At. Spectrosc. **92**, 60–69 (2014).
46. R. D. Cowan and G. H. Dieke, "Self-Absorption of Spectrum Lines," Rev. Mod. Phys. **20**(2), 418–455 (1948).
47. C. Aragón and J. A. Aguilera, "Characterization of laser induced plasmas by optical emission spectroscopy: a review of experiments and methods," Spectrochim. Acta B At. Spectrosc. **63**(9), 893–916 (2008).
48. L. J. Radziemski and D. A. Cremers, *Handbook of Laser Induced Breakdown Spectroscopy*, (John Wiley & Sons, 2006).

1. Introduction

The ability to control materials composition is decisive in obtaining reliable characteristics and performance. In particular, non-stoichiometry has profound consequences on the physical properties of multinary crystalline materials, and has been, for this reason, a long-standing research topic in the fields of electron [1–4] and phonon transports [5–9], magnetism [5, 10, 11] and optics [12–14]. The example of transparent ceramic materials used as specialty optical components [12, 13, 15–19] is no exception to this and color centers [20], charge carrier trapping sites [21] and light-scattering phases [22] induced by non-stoichiometry defects have largely been documented. Whether the result of imperfect powder preparation (e.g. slight weighing errors due to water absorption on high surface-area powders, inhomogeneous co-precipitation of precursors with distinct solubility constants, contamination by grinding media during blending), thermal decomposition during high-temperature sintering [23, 24] or because of unbalanced condensation rates, as in the synthesis of chemically-vapor deposited (CVD'ed) ceramics [25], composition-control poses severe challenges to the consistent fabrication of ceramics with high optical quality. It has been shown, for example, that the solid-solution range for the Yttrium Aluminum Garnet (YAG, $Y_3Al_5O_{12}$) [26, 27], a material widely used as laser gain medium [12, 28], phosphor [29] and scintillator [20], lies within $(5/3\text{-}0.03) < Al/Y < (5/3 + 0.008)$ [20, 30]. From a quality assurance standpoint, as well as for defect-engineering purposes [20], such tight tolerances demand flexible analytical techniques capable of discerning the ratio of major elements with sufficient accuracy.

In the past, nonstoichiometry in YAG samples has been investigated by X-ray diffraction [27], THz spectroscopy [31], and optical spectroscopy [20, 32]. However, the non-monotonic relationship between the Al/Y molar ratio and the instrumental response of the first two techniques and the specific methodoly of the latter limit their applicability for general quantitative assessments. In this letter, we report on the use of Laser-Induced Breakdown Spectroscopy (LIBS) for the quantification of non-stoichiometry in YAG ceramics. This optical emission spectroscopy technique consists in igniting a micro-plasma on the surface of a sample using a focused high-energy pulsed laser. At a given plasma temperature and electronic density, the atomic emission line intensities produced in the plasma are proportional to the number of species undergoing the corresponding transitions, therefore allowing for quantitative elemental analysis. The amount of material ablated in the process is typically in the pico- to nanogram range, and damage to the sample is minimal. The versatility, rapidity and limited sample preparation have all contributed to making LIBS a widely used quantification technique for trace, minor and major elements in a variety of

Optical Materials EXPRESS

matrices, including alloys, composites and ceramics [33–41]. Moreover, LIBS can be adapted to real-time in-*situ* analysis [42].

2. Experimental

To carry out this study, yttrium aluminum oxide ceramic samples of varied compositions near the garnet stoichiometry were prepared by solid-state reaction between alumina and yttria [43]. A 50 g powder mixture of 38 mol% α-Al_2O_3 (Inframat) and 62 mol% Y_2O_3 (Inframat) was ball-milled for 8 hours in the presence of ethanol and alumina balls as a grinding medium. Tetraethoxysilane (Sigma Aldrich) was added to the slurry at a concentration of 0.5 wt % as a sintering additive. After drying, 4 g aliquots of this mixture were blended with controlled quantities of Y_2O_3 to prepare pellets of known composition. Fourteen such samples were prepared with Al/Y molar ratio ranging from 1.600 to 1.684, with step size no more than 0.007. The ratio of 1.667 corresponds to stoichiometric YAG. The degree of hydration of the raw powders and imprecision of the weighing scale (0.2 mg) both contributed to composition uncertainties. The weight loss of the raw powders after calcination at high temperature was determined and accounted for in the fabrication of the ceramic samples. The cumulated error amounted to 0.02% of the nominal compositions (i.e. an order of magnitude smaller than the composition increments between samples). The powder samples were then uniaxially pressed at 20 MPa into pellets and cold isostatically pressed at 200 MPa. After compaction, the pellets were vacuum-sintered in a tungsten-mesh furnace at 1750°C at a pressure of 10^{-6} torr for 2 hours and hot-isostatically pressed at 1700°C at 200 MPa for 2 hours. The samples were subsequently annealed in air at 1400°C for 3 hours. To prevent secondary phase precipitation, cooling rates were maintained above 15°C per minute. Samples within 1.635<Al/Y<1.669 are transparent but translucent outside this composition range.

The spectral line intensities used for quantitative LIBS analysis are affected by several parameters, such as the laser focusing condition, the temporal and spatial stability of the laser pulse, the pulse energy and the plasma stability [44]. Our LIBS system controls these parameters and the detailed description can be found in [45]. The schematics of the apparatus is shown in Fig. 1.

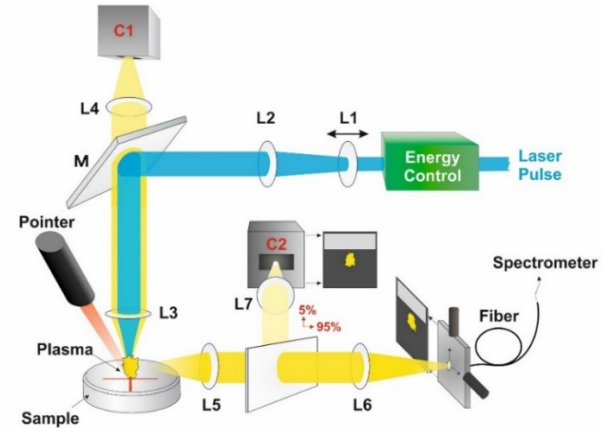

Fig. 1. Schematics of the LIBS setup used in this study.

The laser ablation was carried out at the fourth harmonic of a Q-switched Nd:YAG laser (266 nm, 10 mJ, 5 ns, 10 Hz, Quantel). The laser pulse energy was optimized to produce a stable plasma and maximum ablation for increasing the signal-to-noise ratio and reducing the effect of possible sample heterogeneity. The laser energy is stabilized during the experiments using a combination of a power-meter and a computer controlled attenuator (ATT266 from Quantum Composers). The laser beam is expanded by lenses L1 and L2, with focal lengths of −50 and 100 mm, respectively (Fig. 1). It is then reflected off mirror M towards the

Optical Materials EXPRESS

converging lens L3 (focal length 75 mm). Lenses L1, L2 and L3 are made of fused silica and the dielectric mirror M has a high reflectance at 266 nm and a high transmittance for wavelengths above 300 nm. The beam is focused few hundreds of micrometers under the sample surface which is necessary to prevent air breakdown and produce a stable plasma [45]. The focus point of the laser can be adjusted in height by translating lens L1 horizontally with a motorized translation stage. The ability to control the distance between lens L3 and the sample surface is an important feature of the present system, which guarantees the production of identical fluences and plasma conditions from sample to sample. A laser pointer is directed towards the sample in an oblique fashion and the light reflected off the sample surface is focused by lens L4 onto the CCD camera C1. In the field of view of the camera, the barycenter of the laser spot is very sensitive to the vertical positioning of the sample surface and allows for locking the lens-to-sample distance with an accuracy better than 5 μm. This technique is detailed in [45]. The plasma light is collected by lens L5 of 5 cm focal length and fed into a Czerny-Turner spectrometer (1200 1/mm grating) via an optical fiber consisting of a bundle of 19 fibers of 200 μm core diameter each. The stability of the plasma is monitored by the CCD camera C2 (Thorlab) and the collection fiber is centered with respect to the plasma to account for the shot-to-shot fluctuation of plasma morphology. An intensified charge coupled device (ICCD) camera (Andor Technology) is used for recording the spectra. In this experiment, delay for the laser pulse and the duration of acquisition by the ICCD camera were set to 900 and 1000 ns, respectively.

Because the quantification of major elements by atomic spectroscopy techniques is hampered by self-absorption [46, 47], the non-resonant lines of singly-ionized aluminum (281.61 nm) and yttrium (278.52 nm) were chosen for this analysis [48]. These lines are well isolated and do not suffer any spectral interference. The typical emission spectrum produced by an yttrium aluminum oxide sample, in the 274 to 290 nm spectral window, is shown in Fig. 2. For each sample, 100 spectra were averaged over a 10x10 spot grid to decrease the variance of the measurement and overcome a possible sample heterogeneity. Each individual spectrum was recorded with the accumulation of 10 laser shots at the same position. With this protocol, the duration of a measurement sequence of 100 spectra for a sample was less than 2 minutes. The center to center spacing between neighboring craters was 300 μm.

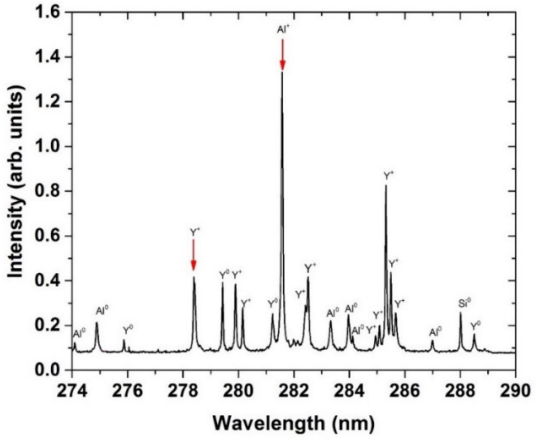

Fig. 2. Typical LIBS spectrum of an yttrium aluminum oxide sample, showing the Al^+ and Y^+ lines used for quantitative analysis. The other spectral features correspond to transitions in neutral and ionized Al and Y species.

3. Results and discussion

Figure 3 shows the correlation between the sample composition and the intensity ratio of the 281.61 nm aluminum and 278.52 nm yttrium lines. The calibration curve has three separate

Optical Materials EXPRESS

trends that correlate to the transparency of the samples. The relationship between the Al/Y intensity and molar ratios is monotonic irrespective of the visual appearance of the samples. The sensitivity of the calibration curve in group I, II and III is 4.31 ± 1.4, 1.53 ± 0.09 and 3.09 ± 0.78, respectively. This correlation is likely due to differences in laser-sample interaction brought about by light-scattering from secondary phases (Al_2O_3 or $YAlO_3$) outside the garnet solid-solution (i.e. outside of group II). As discussed above, the small magnitude of the error bars on the composition axis does not show on the graph. The measured shot-to-shot fluctuations of the Al and Y lines over 1000 spectra is 1%. The propagation of this error into the Al/Y intensity ratio, *r,* and obtained from:

$$\frac{\Delta r}{r} = \left[\left(\frac{\Delta I_{Al}}{I_{Al}} \right)^2 + \left(\frac{\Delta I_Y}{I_Y} \right)^2 \right]^{1/2}$$

where I_{Al} and I_Y designate the line intensities of both Al and Y species, leads to a 1% relative standard deviation on the Al/Y intensity ratio. This allows resolving a 0.3 mol% difference in the Al/Y molar ratio for group II samples. These calibration curves can be used for the precise determination of composition in yttrium aluminum oxide ceramics on either side of the garnet stoichiometric composition.

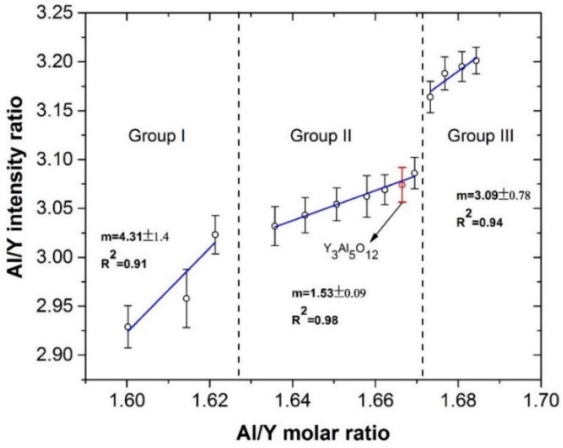

Fig. 3. Variation of the 281.61 nm aluminum and 278.52 nm yttrium line intensity ratios with sample composition. The arrow points to the sample with the stoichiometric garnet phase composition (YAG). The 3 domains (labeled group I, II and III) correspond to the visible appearance of the samples: transparent for group II and translucent for groups I and III. The changes in slope seen in the calibration curves between these groups reflect differences in laser-sample interaction.

4. Conclusion

In summary, we carried out LIBS analysis on fourteen samples of yttrium aluminum oxide ceramics with Al/Y molar ratios near the garnet composition. The intensity ratio of non-resonant spectral lines of singly-ionized aluminum (281.61 nm) and yttrium (278.52 nm) showed a positive correlation with their molar ratios. The smallest difference in molar ratio currently resolved is 0.3 mol%. We believe that such performance will allow better composition control in the fabrication of advanced ceramics of definite line-compounds, including that of high-grade transparent ceramics.